

Microstructure of $\text{Ba}(\text{Mg}_{1/3}\text{Ta}_{2/3})\text{O}_3$ - BaSnO_3 microwave dielectrics

Lai-Cheng Tien^a, Chen-Chia Chou^b, Dah-Shyang Tsai^{a,*}

^aDepartment of Chemical Engineering, National Taiwan University of Science and Technology, Taipei, 106 Taiwan

^bDepartment of Mechanical Engineering, National Taiwan University of Science and Technology, Taipei, 106 Taiwan

Received 10 September 1998; received in revised form 2 October 1998; accepted 3 December 1998

Abstract

Ceramics of $\text{Ba}(\text{Mg}_{1/3}\text{Ta}_{2/3})\text{O}_3$ - BaSnO_3 (BSMT) are synthesized by a two-stage calcination method. Microstructures are analyzed, using X-ray diffractometry, transmission electron microscopy, Raman spectroscopy, and scanning electron microscopy. The addition of BaSnO_3 reduces the cation ordering of $\text{Ba}(\text{Mg}_{1/3}\text{Ta}_{2/3})\text{O}_3$ and its sinterability. Variations in ordered structure with BaSnO_3 content are revealed by the reduction in intensity of the superlattice reflections, the domain size, the c/a ratio, and the shifting and broadening in Raman lines. The relations between microstructure and quality factors of BSMT are discussed. © 1999 Elsevier Science Ltd and Techna S.r.l. All rights reserved.

Keywords: Barium magnesium tantalate; Cation ordering; Tin substitution; Low-loss dielectrics

1. Introduction

Quality factors of complex perovskite ceramics, based on the formula $\text{Ba}(\text{M}_{1/3}\text{Ta}_{2/3})\text{O}_3$ $\text{M}=\text{Mg}$, Zn , were found over 10,000 at microwave frequency around 10 GHz in the 1980s. Since then ceramics of the two compositions have found widespread commercial applications in oscillators and filters in microwave communication [1,2]. Solid solutions of A-site or B-site substitutions were investigated to explore the possibilities of improving dielectric properties [3,4]. A well-known success is 4 mol% BaZrO_3 addition in $\text{Ba}(\text{Zn}_{1/3}\text{Ta}_{2/3})\text{O}_3$ which enhances the quality factor from 10,000 to 14,500 at 10 GHz [5].

Dielectric losses in microwave frequencies are related to the degree of B-site ordering, porosity, secondary phases, and crystal imperfections in ceramics. Among these factors, the degree of ordering is a prominent one [6]. Prolonged sintering or annealing of $\text{Ba}(\text{M}_{1/3}\text{Ta}_{2/3})\text{O}_3$, increases the fraction of ordered structure in crystal, the quality factor is consequently enhanced. Nevertheless, an addition of a small amount of BaZrO_3 depresses the ordering of BZT, the increase of quality factor obviously disobeying the consensus about the

relation between the ordering and the loss factor. Davies and Tong [7] attributed the effect of BaZrO_3 on loss tangent to its stabilization of antiphase boundaries.

B-site substitution of Sn in $\text{Ba}(\text{Mg}_{1/3}\text{Ta}_{2/3})\text{O}_3$ was studied by Matsumoto et al [8]. They reported that the Sn content had a strong influence on the quality factor. High quality factors were recorded in compositions of 0, 10 and 15 mol% Sn. But the composition of 5 mol% Sn had a low quality factor which led to suspicion of the existence of Mg_2SnO_4 or a lower bulk density. In this paper, we revisit the problem and investigate the microstructure and the dielectric properties of $\text{Ba}(\text{Mg}_{1/3}\text{Ta}_{2/3})\text{O}_3$ - BaSnO_3 microwave ceramics.

2. Experimental

Ceramics of composition $(1-x)\text{Ba}(\text{Mg}_{1/3}\text{Ta}_{2/3})\text{O}_3$ - $x\text{BaSnO}_3$ were prepared by a two-stage calcination procedure. Stoichiometric amounts of BaCO_3 (Merck) and SnO_2 (Merck) were dried in an oven, cooled in a desiccator, weighed, and ball milled, using zirconia balls in a polyethylene jar. After 1100°C 3 h calcination, BaSnO_3 was synthesized. Stoichiometric amounts of BaCO_3 , Ta_2O_5 (Aldrich), MgO (Iwatani), and as-prepared BaSnO_3 were mixed in the same way, and calcined at a higher temperature 1300°C for 3 h. The prepared solid solutions of $(1-x)\text{Ba}(\text{Mg}_{1/3}\text{Ta}_{2/3})\text{O}_3$ - $x\text{BaSnO}_3$ were

* Corresponding author. Tel: +886-22737-6618; fax: +886-22737-6644.

E-mail address: tsai@ch.ntust.edu.tw (D.-S. Tsai).

abbreviated as BSMT with x molar fraction of BaSnO_3 or Sn. Calcined BSMT powders were mixed with Darvan C, polyvinyl alcohol, ethylene glycol, and deionized water, and ball milled again for 24 h in a polyethylene jar using zirconia balls. Ceramic disks and short rods were formed by dry pressing, and sintered at 1600°C for various amounts of time.

Sintered density was measured using Archimedes water immersion technique. Sintered specimens (relative density over 95%) were polished and examined by X-ray diffractometry using $\text{CuK}\alpha$ radiation (Dmax-B, Rigaku). Two scanning rates were applied, $1^\circ/\text{min}$ for 2θ range 10 – 40° and $4^\circ/\text{min}$ for 2θ range 10 – 120° . Raman spectra were recorded using a Raman scope (RS-2000, Renishaw Ramanscope) and the excitation light source was a He–Ne laser. The scanning range was 200 – 1000 cm^{-1} .

As-sintered specimens were ground and thermally etched for scanning electron microscopy (SEM) investigations. Average grain sizes were estimated by the linear intercept technique. Selected specimens were ground by hand to a thickness around $150\text{ }\mu\text{m}$. The sample thickness was then reduced to $10\text{ }\mu\text{m}$ in a dimpling machine. An ion miller was used to further reduce the thickness of crystal. After perforation, the sample was bombarded by an ion beam at reduced voltage and tilt angle for several minutes. High-resolution electron microscopy (HRTEM) study was conducted using a transmission electron microscope (Model JEM4000EX, JEOL). The loss tangent of specimen was measured in a resonator cavity of copper metal, using a network analyzer (Model 8722A, Hewlett–Packard).

3. Results and discussion

Bulk densities of BSMT are plotted in Fig. 1. Values of relative density are based on the theoretical density of BMT 7.637 g/cm^3 [9]. As a whole, the addition of BaSnO_3 reduces the sinterability of BMT, which has been identified as a composition of poor sinterability via solid-state-reaction method [10]. The sintered density of BSMT can be improved if the soaking time increases from 30 min to 2 h.

A soaking time longer than 2 h has little effect on the bulk density. Bulk densities of BSMT, synthesized by two-stage calcination, can reach a density over 95% at 1600°C , which is a lower temperature compared with the common sintering temperature 1640 – 1650°C for BMT [8]. The subsequent microstructure study, therefore, is centered on the specimens sintered at 1600°C for 2 h.

Figs. 2(a–d) illustrate the SEM micrographs of BSMT of $x=0.0, 0.05, 0.1, 0.15$, individually. The average grain sizes of these four compositions are listed in Table 1. The grain size of BMT decreases from 1.5 to $0.5\text{ }\mu\text{m}$ with an addition of $5\text{ mol}\%$ BaSnO_3 . Higher

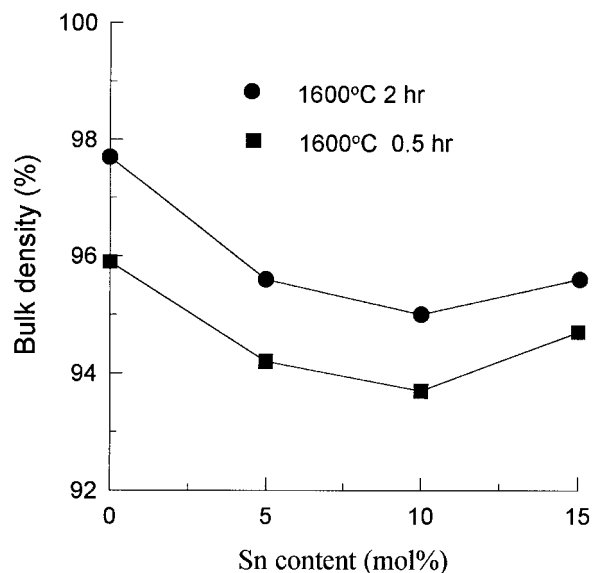


Fig. 1. Bulk densities of BSMT ceramics sintered at 1600°C for 0.5 and 2 h.

Sn content increases the grain size to $3.1\text{ }\mu\text{m}$ ($15\text{ mol}\%$ BaSnO_3). The decrease-then-increase of grain size with Sn content is consistent with Matsumoto's observation [8].

Diffraction patterns of BSMT closely resembles that of BMT in both diffraction angle and intensity, indicated in Fig. 3. Fundamental reflections of specimens of higher Sn content consistently shift to slightly lower angles. Accordingly, lattice constants of c and a both increase with the Sn content, as shown in Table 1. Yet the ratio c/a decreases with the increasing Sn content.

The reduction in c/a ratio is a consequence of the decreasing cation ordering in BSMT. It is known that ordering in B-site cations expands the crystal lattice along $\langle 111 \rangle$ direction of the pseudo-cubic unit cell, and leads to a c/a ratio higher than 1.2247. Intensities of superlattice reflections exhibit the degree of cation ordering. Figs. 4(a) and (b) indicate the XRD scans of BSMT ceramics in the 2θ range of 10° – 40° after sintering for 2 and 24 h. Both intensities of $(100)_h$ and $(200)_h$ superlattice reflection (marked with *) decrease with the Sn content, and increase with the soak time. The subscript h denotes a hexagonal unit cell. The charge and octahedral radius of $\text{Sn}^{4+}0.83\text{ \AA}$, are between those of $\text{Mg}^{2+}0.86\text{ \AA}$ and those of $\text{Ta}^{5+}0.78\text{ \AA}$ [11]. The Sn^{4+} addition reduces the charge difference and the ionic size difference between the two cations Mg^{2+} and Ta^{5+} . Consequently, the long-range ordering of BMT decreases [12]. Prolonged sintering recovers part of the long-range ordering so that reflection $(100)_h$ and $(200)_h$ of 5, 10 mol% BSMT of 24-h sintering appear again in Fig. 4(b).

Since the addition of 4 – $25\text{ mol}\%$ BaZrO_3 in $\text{Ba}(\text{Zn}_{1/3}\text{Ta}_{2/3})\text{O}_3$ is known to promote $1/2 \langle 111 \rangle$ ordered structure, a similar effect is expected on the addition of BaSnO_3 in BMT. The $1/2 \langle 111 \rangle$ ordered structure in

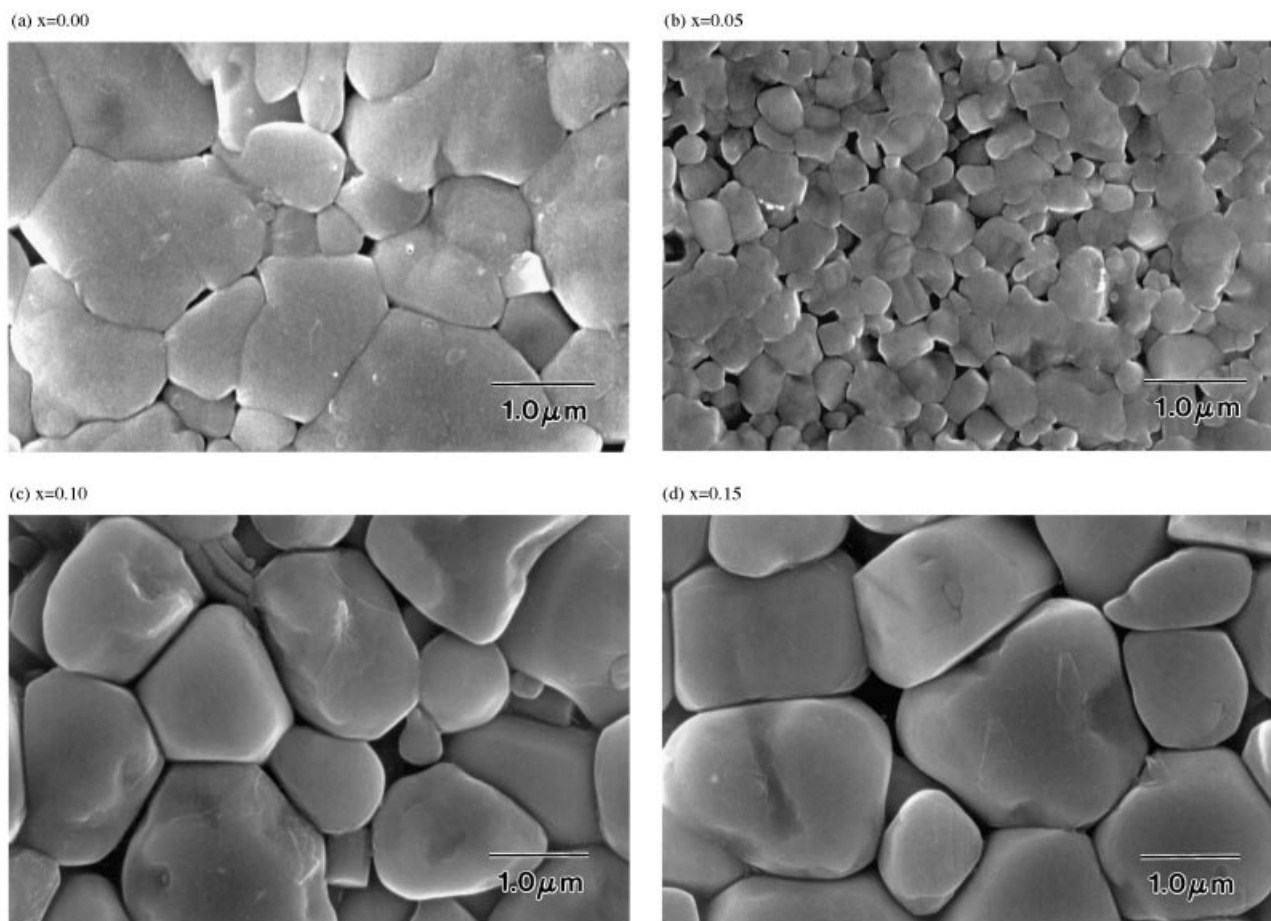


Fig. 2. SEM micrographs of BSMT ceramics sintered at 1600°C for 2 h, (a) 0 mol%, (b) 5 mol%, (c) 10 mol%, (d) 15 mol% BaSnO₃.

BZT could be detected in 1° shifting of superstructure reflection (100)_h, 17.7→18.8° [4,13]. Such a shifting is not observed in X-ray diffraction patterns of BSMT, Fig. 4. Nonetheless, the electron diffraction pattern of BSMT $x=0.05$ indicates that very vague $1/2 <111>$ superlattice spots are imbedded in those $1/3 <111>$ superstructure spots, as illustrated in Fig. 5. The superlattice spots of $1/2 <111>$ ordering are not detected in specimens of BSMT $x=0.10$ and 0.15. It seems that $1/2 <111>$ ordered structure in BSMT is a transient structure that emerges from the composition fluctuations due to Sn substitution.

The $1/3 <111>$ ordered domain size of BSMT sintered at 1600°C for 2 h is estimated from the high-resolution

Table 1
Grain sizes and lattice parameters of BSMT sintered at 1600°C for 2 h

Sn content (mol%)	Grain size (μm)	<i>c</i> (nm)	<i>a</i> (nm)	<i>c/a</i>
0	1.5	0.70843	0.57792	1.2258
5	0.5	0.70911	0.57881	1.2251
10	1.8	0.70924	0.57900	1.2249
15	3.1	0.70991	0.57955	1.2249

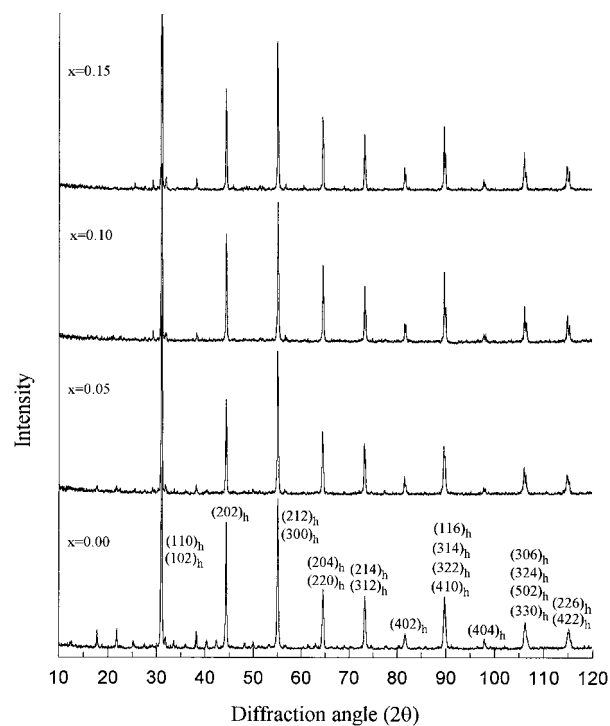


Fig. 3. X-ray diffraction patterns of BSMT sintered at 1600°C for 2 h, 2θ range 10–120°.

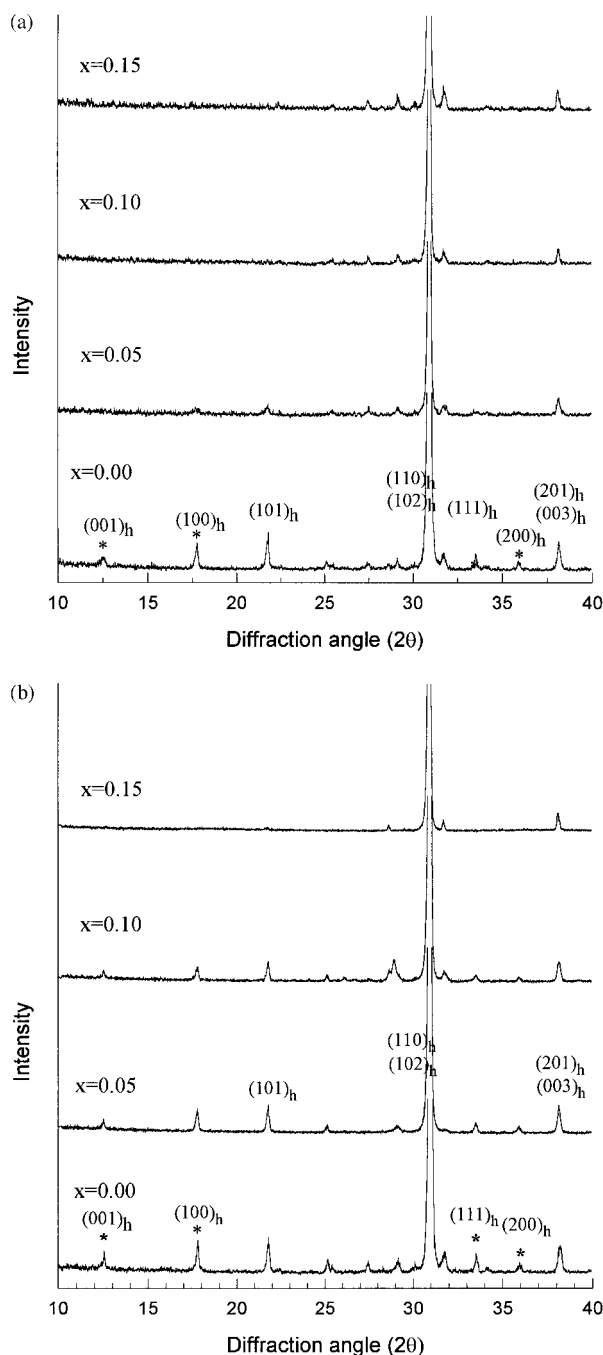


Fig. 4. X-ray diffraction patterns of BSMT sintered at 1600°C for (a) 2 and (b) 24 h, 2θ range 10–40°.

TEM micrographs, shown in Figs. 6 (a–d). The domain size of BMT is around 15–30 nm. Addition of 5 mol% Sn reduces the domain size to 5–10 nm. The ordered domain is not observed for BSMT of $x=0.10$ and 0.15 .

The decline of $1/3 \langle 111 \rangle$ ordered structure in BSMT results in a change in local bonding environment, which is shown in Raman spectra of Fig. 7. The substitution of Sn has a significant effect on three Raman peaks at 379,

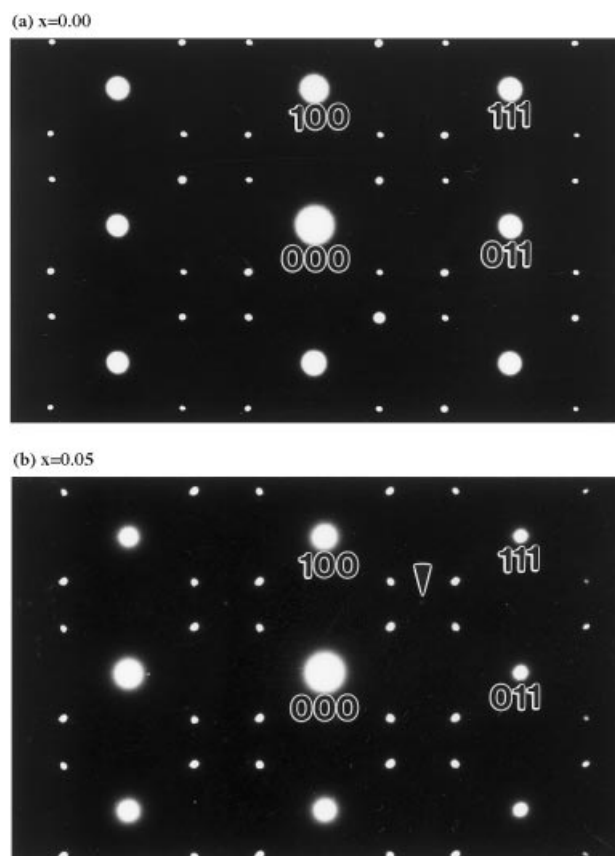


Fig. 5. Selected area electron diffraction patterns of BSMT on [011] zone, showing (a) $1/3 \langle 111 \rangle$ order in BMT, (b) $1/3 \langle 111 \rangle$ and $1/2 \langle 111 \rangle$ order in BSMT of $x=0.05$.

426, and 794 cm^{-1} . With increasing Sn content, the intensity of peak at 379 cm^{-1} shifts to a lower wave number, broadens and vanishes when $x \geq 0.10$. Meanwhile, the two peaks at 426 and 794 cm^{-1} both shift to a lower wave number 422 and 785 cm^{-1} , when $x=0.15$. Also the half linewidth of 422 cm^{-1} peak increases from 10.3 ($x=0.0$) to 14.3 ($x=0.15$) cm^{-1} , that of 785 cm^{-1} increases from 20.0 ($x=0.0$) to 32.0 ($x=0.15$) cm^{-1} . Peaks at 379 and 426 cm^{-1} are related to the torsional-mode vibrations of the B-site cations [14,15]. Apparently intensity decrease and line broadening of these two peaks are closely related to the composition fluctuation in B-site cations that is caused by Sn substitution.

Related dielectric properties of BSMT are listed in Table 2. Although the ordering and bulk densities of specimen $x=0.05$ and 0.10 are somewhat lower, their quality factors are slightly higher than the more dense specimen $x=0.0$ and 0.15 . The result is different from Matsumoto's result that reported much higher quality factors for $x=0.0$ and 0.15 . Table 2 indicates that quality factors of all compositions are higher than 10^4 at microwave frequency 10.4 GHz. The dielectric constant of BSMT is essentially unaffected by the Sn content.

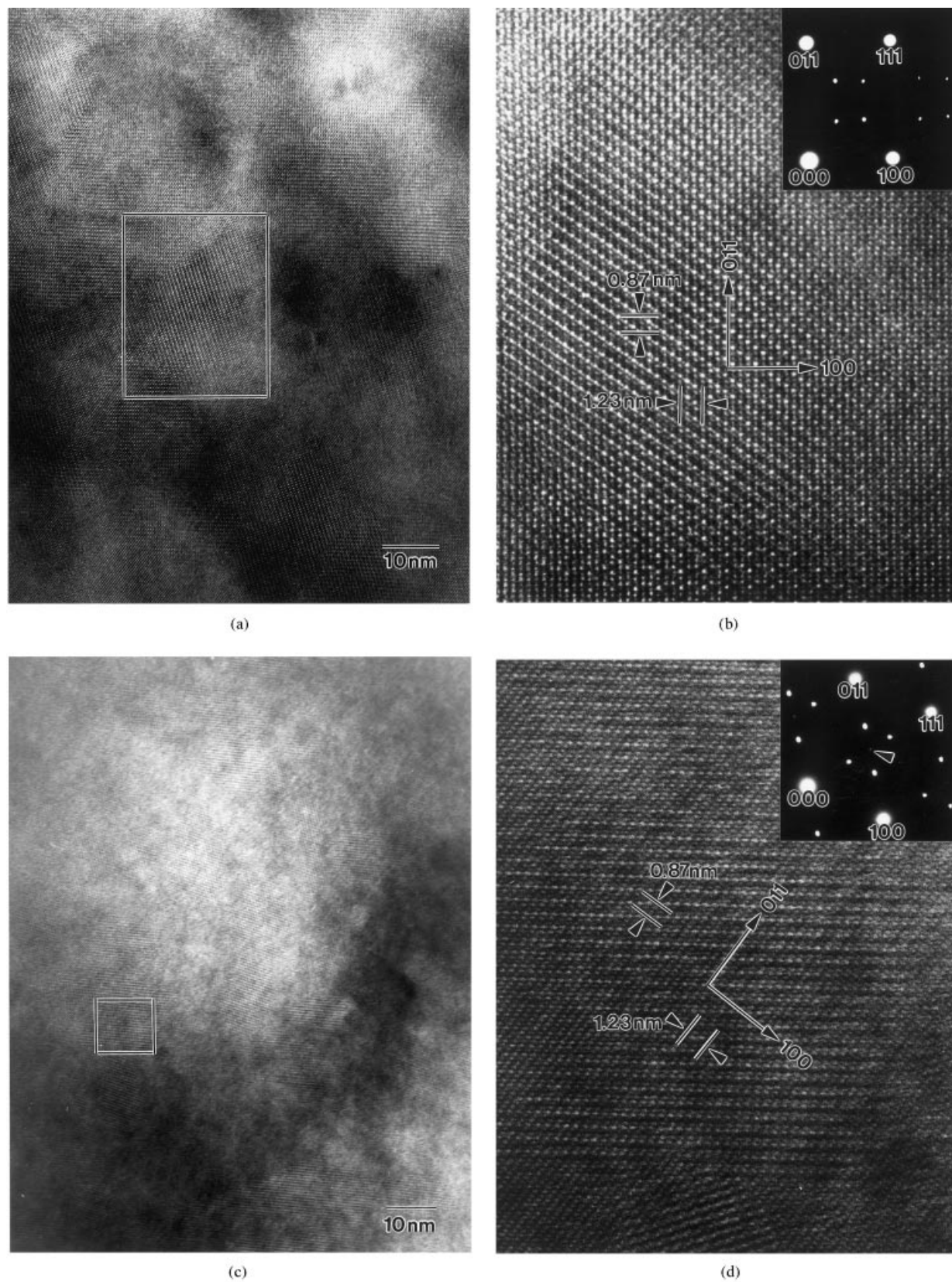


Fig. 6. HRTEM micrographs of ordered microdomains in (a) BMT, (b) magnified image of circled region of (a), (c) BSMT of $x = 0.05$, (d) magnified image of circled region of (c).

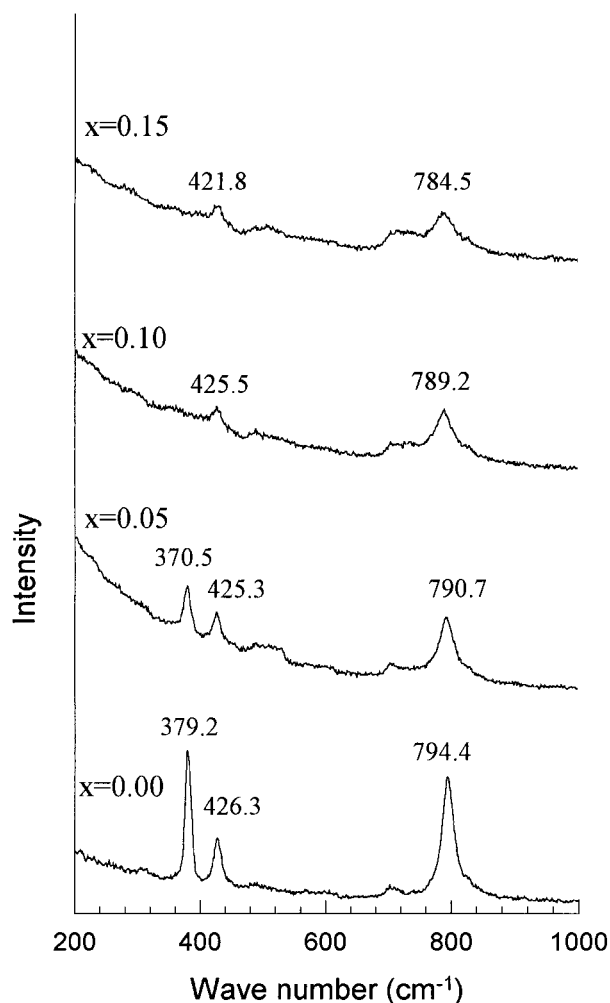


Fig. 7. Raman spectra of BSMT sintered at 1600°C for 2 h, $x=0.0$, 0.05, 0.10, 0.15.

Table 2
Dielectric properties of BSMT sintered at 1600°C for 2 h

Sn content (mol%)	Quality factor (10.4 GHz)	Dielectric constant (10 kHz)
0	$13,300 \pm 3800$	37 ± 1
5	$17,000 \pm 200$	36 ± 1
10	$19,100 \pm 2000$	37 ± 1
15	$11,000 \pm 1300$	36 ± 1

4. Summary

The ordered structure and the dielectric properties of BSMT with 0, 5, 10, 15 mol% Sn are investigated. The substitution of Sn decreases the $1/3 \langle 111 \rangle$ ordering tendency of BMT, which is revealed in superlattice reflections of both X-ray and electron diffraction. The $1/3 \langle 111 \rangle$ ordered domain size decreases from 15–30 nm ($x=0.0$) to 5–10 nm ($x=0.05$). The decreasing ordering also causes shifting and broadening in Raman peaks. A different type of $1/2 \langle 111 \rangle$ ordering is also found in

BSMT of $x=0.05$, but its intensity is rather weak. The $1/2 \langle 111 \rangle$ ordering is not found in specimens of higher Sn content or prolonged sintering. The addition of BaSnO_3 decreases the bulk density of BSMT. Nevertheless, the quality factors of BSMT $x=0.05$ and 0.10 are higher than those of samples $x=0.0$ and 0.15. More structure information is needed in clarifying the relation between loss factor and microstructure of BMT [16].

Acknowledgements

The authors wish to express their gratitude to the National Science Council of Taiwan for partial financial support through grant NSC87-2214-E011-010.

References

- [1] W. Wersing, High frequency ceramic dielectrics and their application for microwave components, in: Electronic Ceramics, B.C.H. Steele (Ed.), Elsevier Applied Science, London, 1991, pp. 67–119.
- [2] A.J. Moulson, J.M. Herbert, Electroceramics, Chapman and Hall, London, 1990 (Chapter 5).
- [3] C.C. Lee, C.C. Chou, D.S. Tsai, Effect of La/K A-site substitutions on the ordering of $\text{Ba}(\text{Zn}_{1/3}\text{Ta}_{2/3})\text{O}_3$, J. Am. Ceram. Soc. 80 (1997) 2885–2890.
- [4] L. Chai, P.K. Davies, Formation and structural characterization of 1:1 ordered perovskites in the $\text{Ba}(\text{Zn}_{1/3}\text{Ta}_{2/3})\text{O}_3$ - BaZrO_3 system, J. Am. Ceram. Soc. 80 (1997) 3193–3198.
- [5] H. Tamura, T. Konoike, Y. Sakabe, K. Wakino, Improved high-Q dielectric resonator with complex perovskite structure, J. Am. Ceram. Soc. 67 (1984) C-59-C-61.
- [6] D.A. Sagala, S. Nambu, Microscopic calculation of dielectric loss at microwave frequencies for complex perovskite $\text{Ba}(\text{Zn}_{1/3}\text{Ta}_{2/3})\text{O}_3$, J. Am. Ceram. Soc. 75 (1992) 2573–2575.
- [7] P.K. Davies, J. Tong, Effect of ordering-induced domain boundaries on low-loss $\text{Ba}(\text{Zn}_{1/3}\text{Ta}_{2/3})\text{O}_3$ - BaZrO_3 perovskite microwave Dielectrics, J. Am. Ceram. Soc. 80 (1997) 1727–1740.
- [8] H. Matsumoto, H. Tamura, K. Wakino, $\text{Ba}(\text{Mg,Ta})\text{O}_3$ - BaSnO_3 high-Q dielectric resonator, Jpn J. Appl. Phys. 30 (1991) 2347–2349.
- [9] S. Nomura, Ceramics for microwave dielectric resonator, Ferroelectrics 49 (1983) 61–70.
- [10] X.M. Chen, Y. Suzuki, N. Sato, Sinterability improvement of $\text{Ba}(\text{Mg}_{1/3}\text{Ta}_{2/3})\text{O}_3$ dielectric ceramics, J. Mater. Sci.: Mater. in Electron. 5 (1994) 244–247.
- [11] R.D. Shannon, Revised effective ionic radii and systematic studies of interatomic distances in halides and chalcogenides, Acta Cryst. A32 (1976) 751–767.
- [12] F. Galasso, J. Pyle, Ordering in compounds of the $\text{A}(\text{B}^{0.33}\text{Ta}_{0.67})\text{O}_3$ type, Inorg. Chem. 2 (1963) 482–484.
- [13] C.C. Lee, C.C. Chou, D.S. Tsai, Variation in the ordering of $\text{Ba}(\text{Zn}_{1/3}\text{Ta}_{2/3})\text{O}_3$ with A-site substitution, Ferroelectrics 206–207 (1998) 293–305.
- [14] K. Tochi, N. Takeuchi, S. Emura, Two-mode behavior in complex perovskite materials, J. Am. Ceram. Soc. 72 (1989) 158–160.
- [15] K. Tochi, T. Ohagaku, N. Takeuchi, Long-wavelength phonons and effective charges in complex perovskite compounds $\text{Ba}(\text{Mn}_{1/3}\text{Ta}_{2/3})\text{O}_3$ and $\text{Ba}(\text{Ni}_{1/3}\text{Ta}_{2/3})\text{O}_3$, J. Mater. Sci. Lett. 8 (1989) 1331–1333.
- [16] H.J. Youn, K.Y. Kim, H. Kim, Microstructural characteristics of $\text{Ba}(\text{Mg}_{1/3}\text{Ta}_{2/3})\text{O}_3$ ceramics and its related microwave dielectric properties, Jpn J. Appl. Phys. 35 (1996) 3947–3953.